A Dynamic Response Model for Explaining the Dynamic Characteristics of a Non-Contact Electromechanical-Magnetic Coupler System

Shaoqing Zheng, Chaojun Yang, Zhenyao tang, Baiqing Liu

Abstract—**In order to determine the variation law of speed and torque along with time during the start-up and speed-regulation processes for a non-contact electromechanical magnetic coupler system (EMCS), a dynamic response model is proposed. Initially, the torques of the motor, magnetic coupler, and load are considered as functions of speed, then several motion equations are established. By numerical integration, the variations of input and output speeds along with time are obtained, allowing the calculation of input and output torques. Then both the start-up and speed regulation dynamic characteristics at different air gap thicknesses are analyzed using the proposed model. Finally, theoretical analysis results are compared with experimental data, demonstrating the model's accuracy.**

Index Terms—**Dynamic response model, electromechanical magnetic coupler, start-up characteristic, speed regulation characteristic.**

I. Introduction

Asynchronous magnetic coupler, a new type of transmission device, offer many advantages such as reliable structure, convenient installation, low cost, energy saving, environmental friendliness and so on [1-3]. They are widely used in applications which require flexible or non-contact transmission, such as mining, electric power generation, and other fields [4-6].

Previous studies on asynchronous magnetic couplers mainly focused on their performance. Early analytical methods could analyze the magnetic field and performance by simplifying the 3D model into a 2D layer model, but these methods required intensive computation and could not handle complex geometries [7-8]. Therefore, both the magnetic equivalent circuit method [9-11] and the magnetic vector potential method [12-14] were developed to overcome these drawbacks in accuracy and universality. For instance, literature[9] analyzed the magnetic field of the magnetic coupler using the magnetic equivalent circuit method and derived expressions for air gap magnetic density and electromagnetic torque. In literature [10], a new equivalent magnetic circuit model that considers eddy current effects was proposed by introducing a branch magnetic circuit for the reaction magnetic flux. In literature[13], a calculation model for predicting the performance of magnetic couplers in both steady-state and transient conditions was presented, demonstrating good accuracy at small slip speeds.

However, current studies primarily focus on the performance of the magnetic couplers themselves, particularly in stable states, with little research on the performance variation during the transition from the unstable to stable state. Literature [15-20] studied the variation of output torque along with time during the operation of magnetic couplers. In reality, the input speed and torque vary with the changes of load and air gap magnetic density, and the range of this variation is influenced by the mechanical characteristics of the motor, magnetic coupler, and load.

To address these issues, a dynamic response model is established for the electromechanical-magnetic coupler system in this paper. This model can be used for predicting the torques, accelerations, and rotational speeds of the input and output during the start-up and speed regulation processes. Additionally, the variation of input speed versus air gap thickness in the stable state can be determined as well.

II. Theoretical Model of EMCS

A. Structure and Torque Analysis of EMCS

Fig. 1 illustrates the structure of a non-contact EMCS, comprising a motor, a magnetic coupler (including an input and output rotor), and a load. The motor is connected to the input rotor, meanwhile the load is connected to the output rotor. The input rotor is equipped with several permanent magnets (PMs), while the output rotor is equipped with a conductor. The output speed is adjustable by regulating the axial air gap distance between this two rotors.

Due to magnetic driving devices transmission torque without contact, the input and output rotors of the coupler operate in different states during actual operation process. Therefore, the kinematic analysis of the system can be divided into two parts: the input and output. The input operates under the effect of both the motor torque (T_M) and the electromagnetic torque (T_{MC}) of the magnetic coupler. Similarly, the output operates under the effect of both the electromagnetic torque (T_{MC}) and the load torque (T_L).

Manuscript received June 29, 2024; revised Mar. 03, 2025.

This work was supported by National Natural Science Foundation of China (Grant No. 51875254) and National Key Laboratory of High-end Equipment Mechanical Transmission Open Fund (SKLMT-MSKFKT-202331).

Shaoqing Zheng is a PhD candidate of School of Mechanical Engineering, Jiangsu University, Zhenjiang, Jiangsu, 212013, China. (Corresponding author phone: +8618825135086; e-mail: zsq2350594@126.com).

Chaojun Yang is a professor of School of Mechanical Engineering, Jiangsu University, Zhenjiang, Jiangsu, 212013, China. (e-mail: yangchaojung@ujsu.edu.cn).

Zhenyao tang is a senior engineer of Guangzhou Special Equipment Testing Institute, Guangzhou, Guangdong, 510000, China. (e-mail: 1345162752@qq.com).

Baiqing Liu is a senior engineer of Guangzhou Special Equipment Testing Institute, Guangzhou, Guangdong, 510000, China. (e-mail: huli217@126.com).

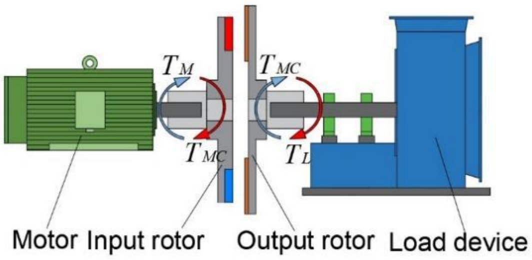

Fig. 1. Structure of EMCS

The dynamic response model requires expressions of the motor torque, electromagnetic torque, and load torque. Mechanical characteristics reflect the relationship between torque produced by the machine and rotational speed. Therefore, the relationship between motor torque (T_M) and input speed (n_{in}) can be expressed by polynomial fitting of the mechanical characteristics:

$$T_M = \sum_{i=1}^{n} p_i (\mathrm{n}_{\mathrm{in}})^{n-i} \tag{1}$$

Wherein p_i are the polynomial coefficients, i and n are natural numbers.

The torque of the magnetic coupler is produced by both the magnetic field of the magnets and the induced magnetic field generated by eddy currents. The induced magnetic field is related to the slip speed of the two rotors. The relationship curve between the electromagnetic torque (T_{MC}) and the slip speed (k) is obtained through finite element simulation and fitted as follows:

$$T_{MC} = \sum_{\mathrm{j}=1}^{\mathrm{n}} \mathrm{p}_{\mathrm{j}} (k)^{\mathrm{n-j}} \tag{2}$$

Wherein p_j are the polynomial coefficients, j is natural numbers, $k = n_{in} - n_{out}$.

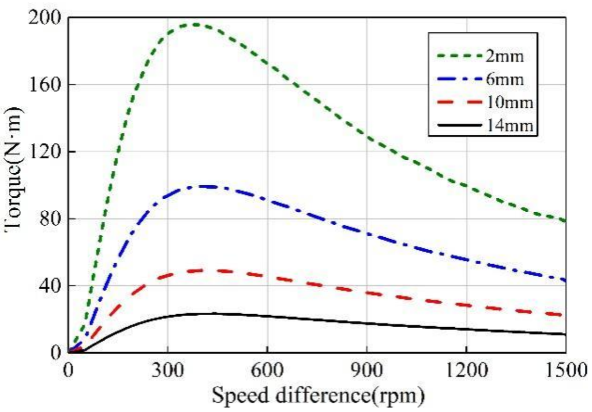

Fig. 2. The relationship between electromagnetic torque and speed difference

For load devices, various production equipment exhibit different load characteristics, categorized into three typical types: constant torque load, variable torque load, and constant power load. The load torque expressions for these types are:

$$T_L = c_1 \quad \text{(constant torque load)} \tag{3}$$

$$T_L = k_2 n_{\mathrm{out}}^{\ 2} \quad \text{(variable torque load)} \tag{4}$$

$$T_L = 30P_3/(\pi n_{\mathrm{out}}) \quad \text{(constant power load)} \tag{5}$$

Wherein c_1 is the load torque of the constant torque load, k_2 is the variable load factor of the variable torque load, P_3 is the power of the constant power load.

B. Dynamic Response Model

Considering the non-contact characteristics of the magnetic coupler, the rotational inertia of the output is unnecessary for motion analysis of the input. The motion equations for the input and output can be expressed as:

$$T_M - T_{MC} = \frac{J_{in}\pi}{30}\frac{dn_{in}}{dt} \tag{6}$$

Wherein J_{in} is the rotational inertia of the input, n_{in} is the input speed.

Similarly, the motion equation of the output can be expressed as:

$$T_{MC} - T_L = \frac{J_{out}\pi}{30}\frac{dn_{out}}{dt} \tag{7}$$

Wherein J_{out} is the rotational inertia of the output, n_{out} is the output speed.

Accelerations of the input and output rotors are given respectively by:

$$\begin{cases} a_{\mathrm{in}} = \dfrac{dn_{\mathrm{in}}}{dt} = \dfrac{30\left(T_M - T_{MC}\right)}{J_{\mathrm{in}}\pi} \\ a_{\mathrm{out}} = \dfrac{dn_{\mathrm{out}}}{dt} = \dfrac{30\left(T_{MC} - T_L\right)}{J_{\mathrm{out}}\pi} \end{cases} \tag{8}$$

Assuming the coupler starts to adjust the speed at time 0, the variations of input and output speed from time 0 to time t are:

$$\begin{cases} \vartriangle n_{\mathrm{in}} = \int_0^t a_{\mathrm{in}} dt \\ \vartriangle n_{\mathrm{out}} = \int_0^t a_{\mathrm{out}} dt \end{cases} \tag{9}$$

Substituting equations (1) ~ (5) into equation (9), then it can be re-expressed as

$$\begin{cases} \vartriangle n_{\mathrm{in}} = \dfrac{30}{J_{\mathrm{in}}\pi}\int_0^t \left(\sum\limits_{i=1}^{n} \mathrm{p}_i (n_{\mathrm{in}})^{n-i} - \sum\limits_{j=1}^{n} p_j (k)^{n-j} \right) dt \\ \vartriangle n_{\mathrm{out}} = \dfrac{30}{J_{\mathrm{out}}\pi}\int_0^t \left(\sum\limits_{j=1}^{n} p_j (k)^{n-j} - f_3\left(n_{\mathrm{out}}\right) \right) dt \end{cases} \tag{10}$$

Wherein $f_3\left(n_{\mathrm{out}}\right)$ represents the torque under the condition of three types load devices and can be given by

$$f_3\left(n_{\mathrm{out}}\right) = \begin{cases} c_1 & \text{(costant torque load)} \\ k_2 n_{\mathrm{out}}^{\ 2} & \text{(variable torque load)} \\ 30P_3/(\pi n_{\mathrm{out}}) & \text{(costant power load)} \end{cases} \tag{11}$$

The initial values of the input and output speed are 0 when the coupler starts, thus, the dynamic input and output speed n_{in} and n_{out} are given respectively by

$$\begin{cases} n_{\mathrm{in}} = \vartriangle n_{\mathrm{in}} \\ n_{\mathrm{out}} = \vartriangle n_{\mathrm{out}} \end{cases} \tag{12}$$

Assuming that the input and output speed in the steady state are n_{in}' and n_{out}' respectively, then the dynamic input and output speed n_{in} and n_{out} during speed regulation are given respectively by

$$\begin{cases} n_{\mathrm{in}} = n_{\mathrm{in}}' + \vartriangle n_{\mathrm{in}} \\ n_{\mathrm{out}} = n_{\mathrm{out}}' + \vartriangle n_{\mathrm{out}} \end{cases} \tag{13}$$

C. Results of Curve Fitting

In this study, an asynchronous magnetic coupler with 9 pairs of PMs is used for torque and speed transmission. The PMs are magnetized in the axial direction. The mechanical characteristics of the magnetic coupler at different air gap thicknesses are shown in Fig. 2. The Y-132S-4 three-phase asynchronous motor is selected to provide power. For the load devices, c_1, k_2 and P_3 are taken as 10N·m, 1.025×10^{-4} and 3kw, respectively. In addition, J_{in} and J_{out} are taken as 5.27×10^{-2} kg·m^2 and 7.16×10^{-2} kg·m^2 respectively. The mechanical characteristics of the motor and three types load devices are given in Fig. 3.

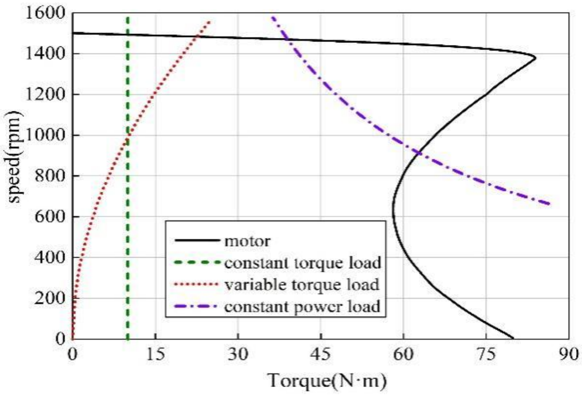

Fig. 3. The mechanical characteristics of the motor and three types load devices

The torque expression of the motor is obtained by curve fitting as:

$$\begin{aligned} T_M =& 2.835\times10^{-24} n_{in}^9 + 1.561\times10^{-20} n_{in}^8 - 3.496\times10^{-17} n_{in}^7 \\ & + 4.086\times10^{-14} n_{in}^6 - 2.647\times10^{-11} n_{in}^5 + 9.255\times10^{-9} n_{in}^4 \\ & - 1.523\times10^{-6} n_{in}^3 + 1.259\times10^{-4} n_{in}^2 - 6.784\times10^{-2} n_{in} + 80.16 \end{aligned} \tag{14}$$

Similarly, the torque expressions of the magnetic coupler at different air gap thicknesses are obtained respectively as:

$$\text{2mm:}\quad \begin{aligned} T_{MC} =& 1.108\times10^{-15}k^6 - 4.964\times10^{-12}k^5 + 7.954\times10^{-9}k^4 \\ & - 4.894\times10^{-6}k^3 + 4.990\times10^{-5}k^2 + 0.8639k \end{aligned} \tag{15}$$

$$\text{6mm:}\quad \begin{aligned} T_{MC} =& 5.696\times10^{-16}k^6 - 2.619\times10^{-12}k^5 + 4.383\times10^{-9}k^4 \\ & - 2.993\times10^{-6}k^3 + 3.591\times10^{-4}k^2 + 0.3660k \end{aligned} \tag{16}$$

$$\text{10mm:}\quad \begin{aligned} T_{MC} =& 2.860\times10^{-16}k^6 - 1.319\times10^{-12}k^5 + 2.220\times10^{-9}k^4 \\ & - 1.538\times10^{-6}k^3 + 2.010\times10^{-4}k^2 + 0.1745k \end{aligned} \tag{17}$$

$$\text{14mm:}\quad \begin{aligned} T_{MC} =& 1.344\times10^{-16}k^6 - 6.248\times10^{-13}k^5 + 1.064\times10^{-9}k^4 \\ & - 7.553\times10^{-7}k^3 + 1.205\times10^{-4}k^2 + 7.756\times10^{-2}k \end{aligned} \tag{18}$$

Assuming the initial values of n_{in} and n_{out} are 0.1rpm and 0rpm respectively in start-up process,which are steady-state values in the speed regulation process, then the variations of n_{in} and n_{out} along with time can be obtained by using numerical analysis software. The dynamic response model, combined with the torque expressions, allows for calculating the variations in input and output torque and acceleration over time.

D. Starting Dynamic Characteristics of Magnetic Coupler

Torque, acceleration, speed, and start response time under the condition both of constant torque load and variable torque load are analyzed. However, constant power loads exhibit constant power characteristics during operation, so dynamic characteristics analysis for start-up is unnecessary.

Fig. 4 and Fig.5 show the variations of speed and torque for the magnetic coupler over time in the air gap thicknesses of 10 mm and 14 mm under constant torque load. When the air gap thickness is 10 mm, the input and output speeds reach a stable operation stage almost simultaneously. However, at 14 mm, the input speed stabilizes quickly while the output speed stabilizes slowly.

The reason is found by analyzing the torque curve. Before reaching the critical speed difference, the electromagnetic torque increases with the speed difference increase, but after exceeding the critical speed difference, it will decrease as the speed difference increases. When the air gap is 14 mm, the input speed rises much faster than the output speed, causing the speed difference to quickly exceed the critical value, but the electromagnetic torque will gradually decrease until the input end is close to a stable state, the speed difference drops, and the electromagnetic torque increase again.

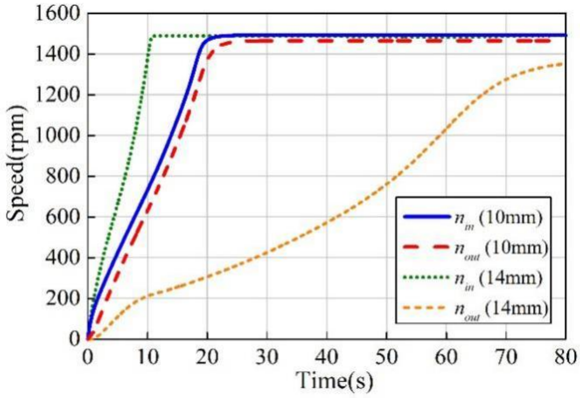

Fig. 4. Speed variation curve under constant torque load

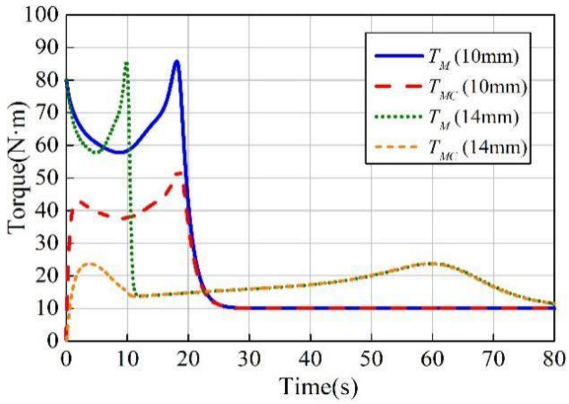

Fig. 5. Torque change curve under constant torque load

Fig. 6 and Fig.7 show the variations of speed and torque in air gap thicknesses of 10 mm and 14 mm under variable torque load with a coefficient of 1.025×10^{-5}. Compared with constant torque load, the magnetic coupler exhibits similar starting dynamic characteristics under variable torque load as well. However, variable torque load has a gradual loading process, so the time that required for input and output speeds to stabilize is not significantly extended.

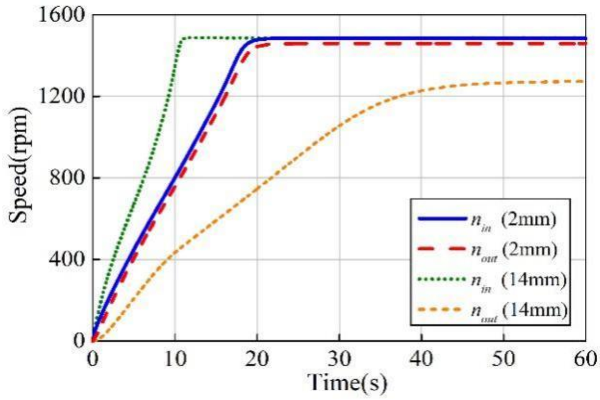

Fig. 6. Speed change curve under variable torque load

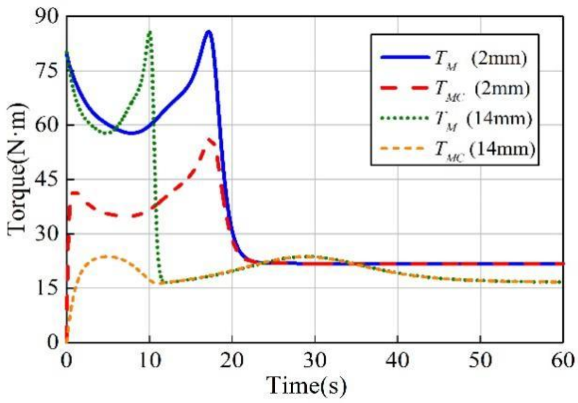

Fig. 7. Torque change curve under variable torque load

E. Speed regulation dynamic characteristics of magnetic coupler

Using the dynamic response model and numerical analysis software, the speed curves for input and output speeds during speed regulation to a 10 N·m constant torque load are obtained, as shown in Fig. 8.

When the air gap thickness changes, the speed difference remains constant due to inertia, but the electromagnetic torque varies, which causes the system state to shift from stable to unstable. For example, when the air gap thickness is adjusted from 2 mm to 14 mm, the input speed rises briefly before returning to the original steady-state speed, while the output speed decreases. Conversely, when it is adjusted from 14 mm to 2 mm, the input speed decreases briefly before returning to the original steady-state speed, and the output speed increases. Comparing these scenarios, the input speed's amplitude changes less and stabilizes more quickly in the former case.

The dynamic response model is benefit to gain the input speed in different air gap thicknesses, and the input speed range in air gap thicknesses shifting from 2 mm to 14 mm can be recorded when the system is stable. Numerical analysis software calculates constant torque, variable torque, and constant power load scenarios, shown in Fig.9. It is evident that as the air gap thickness increases, the steady-state input speed remains constant under constant torque load, slightly increases under variable torque load, and decreases slightly under constant power load. The output speed decreases significantly under all three load types.

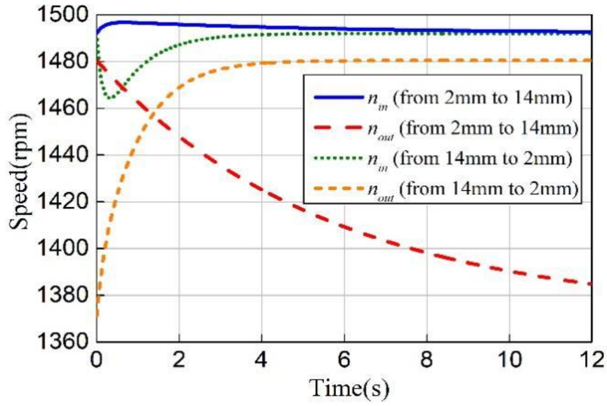

Fig. 8. Speed curve during speed regulation under constant torque load

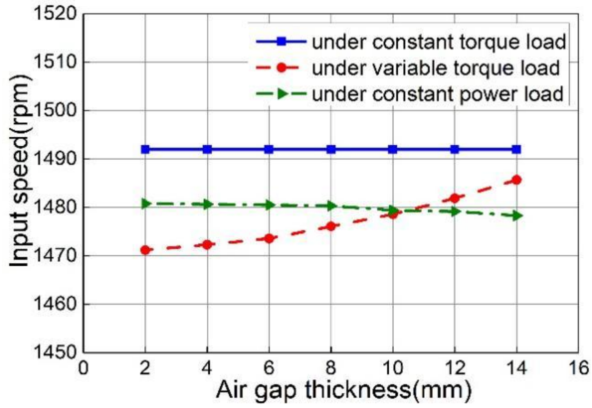

Fig. 9. Curve of input speed with air gap thickness

III. EXPERIMENTAL VERIFICATION

For verification the dynamic response model, a test platform is built for testing the electromagnetic coupler system's performance under different load conditions.

A. Experimental prototype and experimental platform

Fig. 10 and Fig. 11 show the electromagnetic coupler system under constant torque and variable torque load conditions respectively. These platform include the motor, sensor, magnetic coupler, sensor, and magnetic powder brake (or fan).

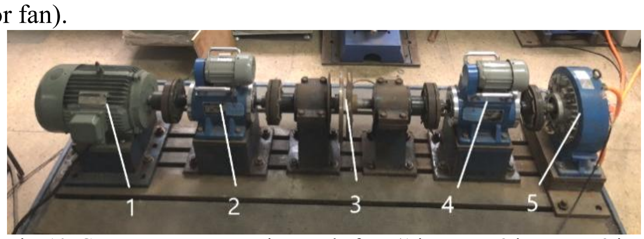

Fig. 10. Constant torque experiment platform(1 is motor; 2 is sensor; 3 is Electromechanical-Magnetic coupler; 4 is sensor; 5 is magnetic powder brake for constant torque load).

Fig. 11. Variable torque experiment platform(1 is motor; 2 is sensor; 3 is Electromechanical-Magnetic coupler; 4 is sensor; 5 is fan for variable torque load).

The mechanical characteristic curves of magnetic couplers with different speed are shown in Fig.12. By comparing different input speed states, it can be seen that when the speed difference is less than 110 rpm, the theoretical and experimental values are basically the same. When the speed difference is more than 110 rpm, the calculated value gradually exceeds the experimental value and the error is large. This error is due to the well-known magnetic field coupling, which can no longer be overlooked for speed difference more than 110rpm. Since the prototype has not been replaced, the maximum output torque does not change with the change of input speed.

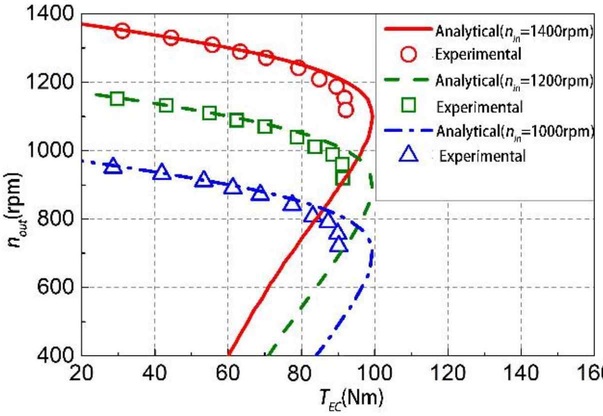

Fig.12. The mechanical characteristic curves of magnetic couplers with different speed (g=6mm)

B. Speed and torque changes during startup

The Electromechanical-Magnetic coupler is connected to the magnetic powder brake after zero-load calibration, then the air gap thickness is adjusted to 6 mm. The output torque of the magnetic powder brake maintains at 10 N·m by adjusting the steady current power supply. The motor is started and maintained the frequency at 50 Hz. Then the value change of speed and torque for both input and output is recorded in every second. Above test process is repeated in the 14 mm air gap thickness, then the measured values are recorded during the startup process.

Some simulations about input , output speed and torque are done by using the dynamic response model, as shown form Fig. 12 to Fig.15.The output speed remains below the critical speed difference, and the torque fluctuation of the output is similar to the input. The trends of input and output speed, and the time required to reach stable operation, which are consistent. Due to some factors such as friction and wind resistance, the measured values are generally smaller than the simulated one.

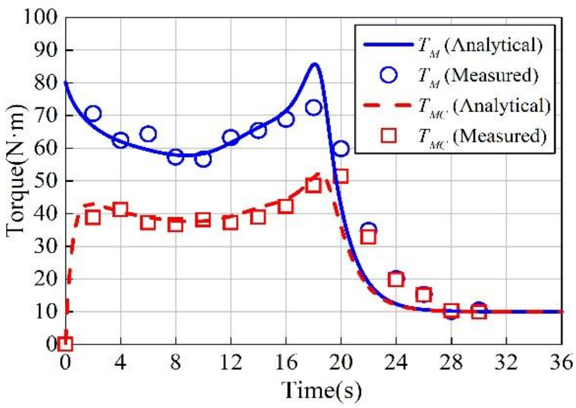

Fig. 13. Torque change curve at the start of air gap thickness 6mm

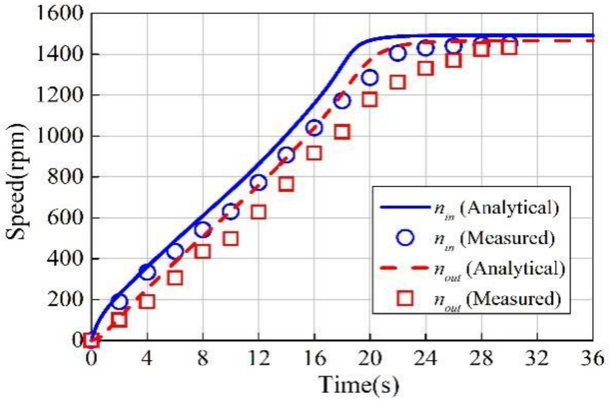

Fig. 14. Speed variation curve at the start of air gap thickness 6mm

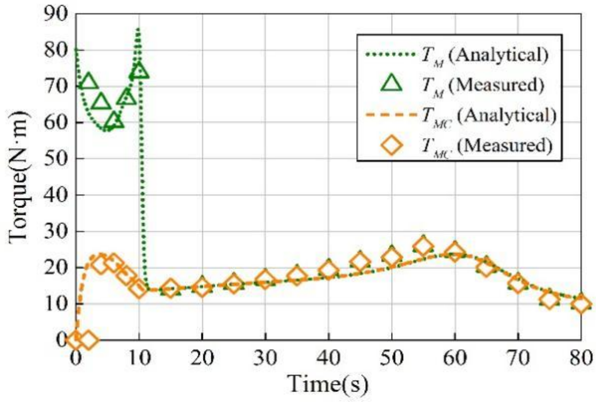

Fig. 15. Torque change curve at the start of air gap thickness 14mm

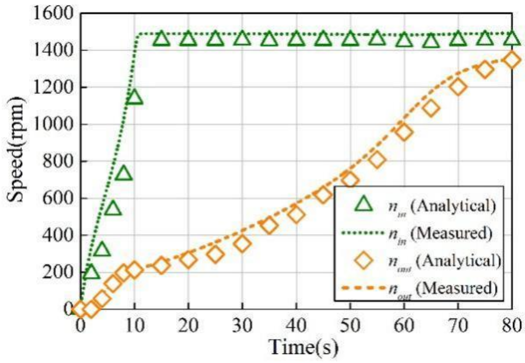

Fig. 16. Speed variation curve at the start of air gap thickness 14mm

C. Steady speed change at different air gap thickness

The motor is started and maintained the frequency at 50 Hz. Then the air gap thickness of the magnetic coupler is adjusted at the value of 4 mm, 6 mm, 8 mm, 10 mm, and 12 mm respectively. Subsequently, as shown in Fig.6, input speed measurement values are recorded after the system stabilizes under constant torque and variable torque loads.

Due to the function of friction and wind resistance, the theoretical stable input speed values differ from experimental values. However, the trend line shows the input speed changes with air gap thickness variation. Under constant torque load, the input speed remains constant, while under variable torque load, the input speed increases as the air gap thickness increases.

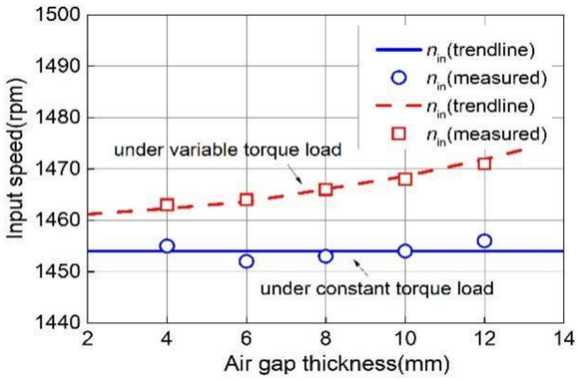

Fig. 17. Curve of input speed with air gap thickness

IV. Conclusion

This paper presents a dynamic response model for the electromagnetic coupler system of a non-contact machine. The model predicts changes in input speed, torque, output speedand torque over time during start-up and speed regulation processes.

The dynamic response model reveals two start-up states for the coupler. In one state, the speed difference remains below the critical value, with similar rising trends for both input and output speeds but large output torque. In the other state, the input speed increases rapidly, which causes the speed difference to exceed the critical value, resulting in output speed rise slowly and small torque fluctuation.

Comparing stabilized input speeds under different loads, the steady-state input speed remains constant under constant torque load, slightly increases under variable torque load, and slightly decreases under power load. The steady-state output speed decreases significantly under all three load types.

Tests show that the changes of torque and speed are consistent with those predicted by the dynamic response model, validating the model.

References

[1] Tonoli A. “Dynamic characteristics of eddy current dampers and couplers”. Journal of Sound and Vibration, vol. 301, no. 3-5, pp. 576-591, 2007.

[2] Li Y, Lin H, Yang H, et al. “Analytical Analysis of a Novel Flux Adjustable Permanent Magnet Eddy-Current Coupler with a Movable Stator Ring”. IEEE Transactions on Magnetics, vol. 54, no. 3, pp. 1-4, 2018.

[3] Wallace A, Von Jouanne, A Jeffryes, et al. “Performance testing of power electronic and permanent-magnet adjustable-speed drives”. Electric Power Components and Systems, vol. 29, no. 12, pp. 1123–1132, 2001.

[4] WANG Hongqun, YU Peiqing, ZHANG Zhigeng. “Technology development of magnetic transmission application”. Heavy Machinery, vol. 06, pp. 1, 2006.

[5] Caijun L, Jie M, Wujin Z. “Asynchronous Permanent Magnet Coupler Hydraulic Coupler and Performance Analysis”. Applied Mechanics and Materials, vol. 427-429, pp. 429-432, 2013.

[6] A Wallace, A von Jouanne, S Williamson. “Performance Prediction and Test of Adjustable, Permanent-magnet, Load Transmission Systems”. IEEE Transactions On Industry Applications, vol. 3, no. 1, pp. 1648-1655, 2001.

[7] Y. Du, et al. “Equivalent magnetic circuit analysis of doubly salient PM machine with Ⅱ-shaped stator iron core segments”. IEEE Trans. Appl. Supercond., vol. 30, no. 4, 2020, Art. no. 5201505.

[8] Belguerras L, Hadjout L, Mezani S, et al. “Study of HTS Magnetic Coupler Using Analytical and Numerical Computations”. IEEE Transactions on Applied Superconductivity, vol. 24, no. 6, pp. 1-12, 2014.

[9] Mohammadi S, Mirsalim M, et al. “Analytical modeling and analysis of axial-flux interior permanent-magnet couplers”. IEEE Transactions on Industrial Electronics, vol.61, no. 11, pp. 5940, 2014.

[10] Li WY, Huang SR. “Analysis and Design of Hybrid Excitation Claw-pole Generator”. Electric Power Components and Systems, vol. 39, no. 7, pp. 680-695, 2011.

[11] Wang J, Zhu J. “A Simple Method for Performance Prediction of Permanent Magnet Eddy Current Couplers Using a New Magnetic Equivalent Circuit Model”. IEEE Transactions on Industrial Electronics, vol. 65, no. 3, pp. 2487-2495, 2018.

[12] Wang J, Lin H, Fang S, et al. “A general analytical model of permanent magnet eddy current couplers”. Magnetics, IEEE Transactions on, vol. 50, no. 1, pp. 1-9, 2014.

[13] Lubin T, Rezzoug A. “Steady-State and Transient Performance of Axial-Field Eddy-Current Coupler”. IEEE Transactions on Industrial Electronics, vol. 62, no. 4, pp. 2287-2296, 2015.

[14] Yang C, Liu K, Wu Y, et al. “Analysis of Transmission Performance for Asynchronous Magnetic Coupler with Trapezoidal Halbach-Array Permanent Magnet”. International Conference on Mechanical Design. Springer, Singapore, pp.125-138, 2017.

[15] Aberoomand V, Mirsalim M, Fesharakifard R. “Design Optimization of Double-Sided Permanent-Magnet Axial Eddy-Current Couplers for Use in Dynamic Applications”. IEEE Transactions on Energy Conversion, vol. 34, no. 2, pp. 909-920, 2019.

[16] Dai X, Cao JY, Long Y, et al. “Analytical Modeling of an Eddy-current Adjustable-speed Coupling System with a Three-segment Halbach Magnet Array”. Electric Power Components and Systems, vol. 43, no. 17, pp. 1891-1901, 2015.

[17] J. Wang, H. Lin, S. Fang and Y. Huang. “A general analytical model of permanent magnet eddy current couplings”. IEEE Trans. Magn., vol. 50, no. 1, pp. 1-9, 2014.

[18] L. S. Belguerras, S. Mezani, T. Lubin, “Analytical modeling of an axial field magnetic coupler with cylindrical magnets”. IEEE Transactions on Magnetics, vol. 57, no. 2, pp. 1-5, 2021.

[19] C. Kral, A. Haumer, C. Grabner. “Consistent Induction Motor Parameters for the Calculation of Partial Load Efficiencies by Means of an Advanced Simulation Model”. Engineering Letters, vol 18, issue 1, pp. 28-40, 2010.

[20] A. Ghoggal, M. Sahraoui, S.E Zouzou. “ A Comprehensive Method for the Modeling of Axial Air-gap Eccentricities in Induction Motors”. Engineering Letters, vol. 17, issue 2, pp. 45-53, 2009.